

C 55.13: 11530 24

A UNITED STATES
DEPARTMENT OF
COMMERCE
PUBLICATION



NOAA Technical Report NESS 64

U. S. DEPARTMENT OF COMMERCE
National Oceanic and Atmospheric Administration
National Environmental Satellite Service

Radiometric Techniques for Observing the Atmosphere From Aircraft

WILLIAM L. SMITH and WARREN J. JACOB



NOAA TECHNICAL REPORTS

National Environmental Satellite Service Series

The National Environmental Satellite Service (NESS) is responsible for the establishment and operation of the National Operational Meteorological Satellite System and of the environmental satellite systems of NOAA. The three principal offices of NESS are Operations, Systems Engineering, and Research. The NOAA Technical Report NESS series is used by these offices to facilitate early distribution of research results, data handling procedures, systems analyses, and other information of interest to NOAA organizations.

Publication of a report in NOAA Technical Report NESS series will not preclude later publication in an expanded or modified form in scientific journals. NESS series of NOAA Technical Reports is a continuation of, and retains the consecutive numbering sequence of, the former series, ESSA Technical Report National Environmental Satellite Center (NESC), and of the earlier series, Weather Bureau Meteorological Satellite Laboratory (MSL) Report. Reports 1 through 37 are listed in publication NESC 56 of this series.

Reports 1 through 50 in the series are available from the National Technical Information Service (NTIS), U.S. Department of Commerce, Sills Bldg., 5285 Port Royal Road, Springfield, Va. 22151. Price \$3.00 paper copy; \$0.95 microfiche. Order by accession number, when given, in parentheses. Beginning with 51, printed copies of the reports are available through the Superintendent of Documents, U.S. Government Printing Office, Washington, D.C. 20402. Price as indicated. Microfiche available from NTIS (use accession number when available). Price \$0.95.

ESSA Technical Reports

- NESC 38 Angular Distribution of Solar Radiation Reflected From Clouds as Determined From TIROS IV Radiometer Measurements. I. Ruff, R. Koffler, S. Fritz, J. S. Winston, and P. K. Rao, March 1967. (PB-174-729)
- NESC 39 Motions in the Upper Troposphere as Revealed by Satellite Observed Cirrus Formations. H. McClure Johnson, October 1966. (PB-173-996)
- NESC 40 Cloud Measurements Using Aircraft Time-Lapse Photography. Linwood F. Whitney, Jr., and E. Paul McClain, April 1967. (PB-174-728)
- NESC 41 The SINAP Problem: Present Status and Future Prospects; Proceedings of a Conference Held at the National Environmental Satellite Center, Suitland, Maryland, January 18-20, 1967. E. Paul McClain, October 1967. (PB-176-570)
- NESC 42 Operational Processing of Low Resolution Infrared (LRIR) Data From ESSA Satellites. Louis Rubin, February 1968. (PB-178-123)
- NESC 43 Atlas of World Maps of Long-Wave Radiation and Albedo--for Seasons and Months Based on Measurements From TIROS IV and TIROS VII. J. S. Winston and V. Ray Taylor, September 1967. (PB-176-569)
- NESC 44 Processing and Display Experiments Using Digitized ATS-1 Spin Scan Camera Data. M. B. Whitney, R. C. Doolittle, and B. Goddard, April 1968. (PB-178-424)
- NESC 45 The Nature of Intermediate-Scale Cloud Spirals. Linwood F. Whitney, Jr., and Leroy D. Herman, May 1968. (AD-673-681)
- NESC 46 Monthly and Seasonal Mean Global Charts of Brightness From ESSA 3 and ESSA 5 Digitized Pictures, February 1967-February 1968. V. Ray Taylor and Jay S. Winston, November 1968. (PB-180-717)
- NESC 47 A Polynomial Representation of Carbon Dioxide and Water Vapor Transmission. William L. Smith, February 1969. (PB-183-296)
- NESC 48 Statistical Estimation of the Atmosphere's Geopotential Height Distribution From Satellite Radiation Measurements. William L. Smith, February 1969. (PB-183-297)
- NESC 49 Synoptic/Dynamic Diagnosis of a Developing Low-Level Cyclone and Its Satellite-Viewed Cloud Patterns. Harold J. Brodrick and E. Paul McClain, May 1969. (PB-184-612)
- NESC 50 Estimating Maximum Wind Speed of Tropical Storms From High Resolution Infrared Data. L. F. Hubert, A. Timchalk, and S. Fritz, May 1969. (PB-184-611)

(Continued on inside back cover)



U.S. DEPARTMENT OF COMMERCE
Peter G. Peterson, Secretary

NATIONAL OCEANIC AND ATMOSPHERIC ADMINISTRATION
Robert M. White, Administrator

NATIONAL ENVIRONMENTAL SATELLITE SERVICE
David S. Johnson, Director

NOAA Technical Report NESS 64

Radiometric Techniques for Observing the Atmosphere From Aircraft

William L. Smith and Warren J. Jacob

U. S. Depository Copy

WASHINGTON, D.C.
JANUARY 1973

UDC 551.507.352:551.508.21:551.501.7

| | |
|-------|--|
| 551.5 | Meteorology |
| .501 | Methods of observation and computation |
| .7 | Upper air observation methods |
| .507 | Instrument carriers |
| .352 | Aircraft observation |
| .508 | Instruments |
| .21 | Radiometers |

Mention of a commercial company or product does not constitute an endorsement by the NOAA National Environmental Satellite Service. Use for publicity or advertising purposes of information from this publication concerning proprietary products or the tests of such products is not authorized.

CONTENTS

| | |
|--|----|
| Abstract | 1 |
| 1. Introduction | 1 |
| 2. The airborne ITPR | 2 |
| 3. Radiance specification of atmospheric variables | 2 |
| A. Atmospheric temperature profiles | 2 |
| B. Total precipitable water | 4 |
| C. Clear column radiance | 5 |
| D. Cloud height | 7 |
| E. Effective cloud amount | 8 |
| 4. Results | 8 |
| 5. Conclusion | 11 |
| Acknowledgments | 11 |
| References | 12 |

RADIOMETRIC TECHNIQUES FOR OBSERVING THE ATMOSPHERE FROM AIRCRAFT*

William L. Smith and Warren J. Jacob
National Environmental Satellite Service
National Oceanic and Atmospheric Administration
Washington, D. C.

ABSTRACT. Radiometric observations have been made from aircraft with spacecraft prototype instruments to test satellite remote sensing techniques. At the same time these observations have been used to study the problem of remote sensing from aircraft because of its own particular value in providing data in the support of sub-synoptic scale meteorological experiments such as the forthcoming GARP Atlantic Tropical Experiment.

This paper describes aircraft radiometric methods of obtaining clear column radiances, vertical temperature profiles, total precipitable water, and cloud heights and amounts. Questions regarding vertical resolution and accuracy specification as a function of aircraft altitudes are answered. Results obtained using observations made during June 1970 with prototype versions of the Nimbus-E ITPR aboard the NASA CV-990 are presented and discussed. It is concluded that multi-spectral radiometers aboard an aircraft can be effective meteorological observing tools.

1. INTRODUCTION

In this paper we present methods of making meteorological inferences using multi-spectral infrared radiance observations made from an aircraft. In particular, methods are given for obtaining: (1) clear column radiances, (2) the vertical temperature profile from aircraft altitude to the earth's surface, (3) the total precipitable water beneath the aircraft, and (4) the height and amount of any clouds below the aircraft flight level. The techniques are tested using radiance observations obtained by a brassboard version of the Infrared Temperature Profile Radiometer (ITPR) from the NASA Convair 990 aircraft during June 1970. Results presented were obtained from observations during a flight over the Pacific Ocean (from Fairbanks, Alaska to San Francisco, California) in which a cold front was encountered near weather ship "Papa" (50°N, 145°W). These results demonstrate that spectral radiometric measurements are very useful for obtaining a detailed depiction of the atmosphere's meteorological state from an aircraft observation platform.

*Presented at the Conference on Atmospheric Radiation,
Ft. Collins, Colorado, August 7-9, 1972.

2. THE AIRBORNE ITPR

The 1970 airborne ITPR experiment has already been discussed in detail by Smith et al., (1972). Briefly, the ITPR measured the upwelling radiance from the underlying earth and atmosphere in five different spectral regions; one in the rotational water vapor band near $19\mu\text{m}$, three in the $15\text{-}\mu\text{m}$ CO_2 band, and one in the atmospheric window at $11\mu\text{m}$. The detailed spectral response characteristics of the ITPR channels are presented in figure 1.

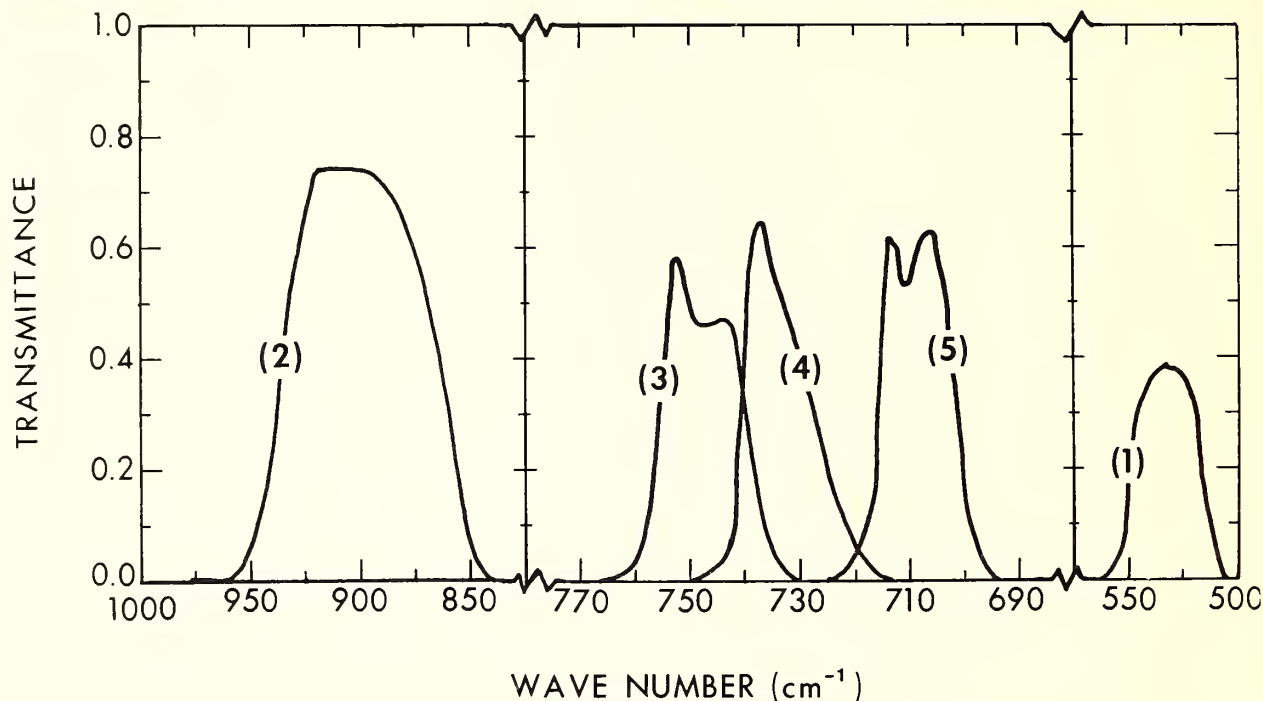


Figure 1.--Measured transmittances of the spectral filters in ITPR channels 1 through 5

3. RADIANCE SPECIFICATION OF ATMOSPHERIC VARIABLES

A. Atmospheric Temperature Profiles

The radiance measured by the ITPR, $I_v(p_a)$, is related to the atmospheric temperature profile through the radiative transfer equation

$$I_v(p_a) = B_v(p_o) \tau_v(p_a, p_o) - \int_{p_a}^{p_o} B_v(p) \frac{d\tau_v(p_a, p)}{dp} dp. \quad (1)$$

$B_v(p)$ is the Planck radiance given by

$$B_v(p) = C_1 v^3 / \left[\exp(C_2 v / T(p)) - 1 \right] , \quad (2)$$

where C_1 and C_2 are constants of the Planck function, and $T(p)$ is the temperature at pressure p . $\tau_v(p_a, p)$ is the transmittance of the atmosphere between the pressure p and the aircraft pressure level p_a , and p_0 denotes the surface pressure.

The solution of (1) for $T(p)$ has been discussed by numerous authors and most of the viable methods have been recently summarized by Fleming and Smith (1972). For the aircraft inference problem the "statistical regression" solution has been adopted. In this solution

$$B_r(p) = \bar{B}_r(p) + \sum_{i=1}^n \alpha_i(p_a, p) \left[R_i(p_a) - \bar{R}_i(p_a) \right] , \quad (3)$$

where $B_r(p)$ is the Planck radiance corresponding to a reference frequency r , chosen to be intermediate to the observation frequency range, and $R_i(p_a)$ is the measured radiance for the i^{th} frequency I_i , normalized to the reference frequency by using the relation

$$R_i = C_1 r^3 / \left[\exp(C_2 r / T_1^B) - 1 \right] , \quad (4)$$

where the brightness temperature T_1^B is given by the inverse Planck function

$$T_1^B = C_2 v_i / \ln \left[(C_1 v_i^3 / I_i) + 1 \right] . \quad (5)$$

The barred quantities denote the means of the statistical sample used to derive the regression coefficients $\alpha_i(p_a, p)$. Once $B_r(p)$ is determined, the temperature profile is calculated using the inverse Planck function in the form

$$T(p) = C_2 r / \ln \left[(C_1 r^3 / B_r(p)) + 1 \right] \quad (6)$$

In this study the regression coefficients were determined from radiances calculated for the heterogeneous sample of 106 atmospheres given by Wark et al. (1962). The transmittance functions needed to calculate the ITPR radiances were taken from Smith et al. (1972). Random errors on the order of 0.25% were added to the calculated radiances to simulate actual radiance observations. The regression coefficients were obtained for aircraft pressure-altitudes of 950 mb to 200 mb in increments of 50 mb. For each aircraft pressure-altitude, regression coefficients relating the aircraft-level temperatures and the "observed" radiances to the temperatures of various levels were determined, using the standard least-squares solution.

Figure 2 shows the resulting standard error of estimate associated with the

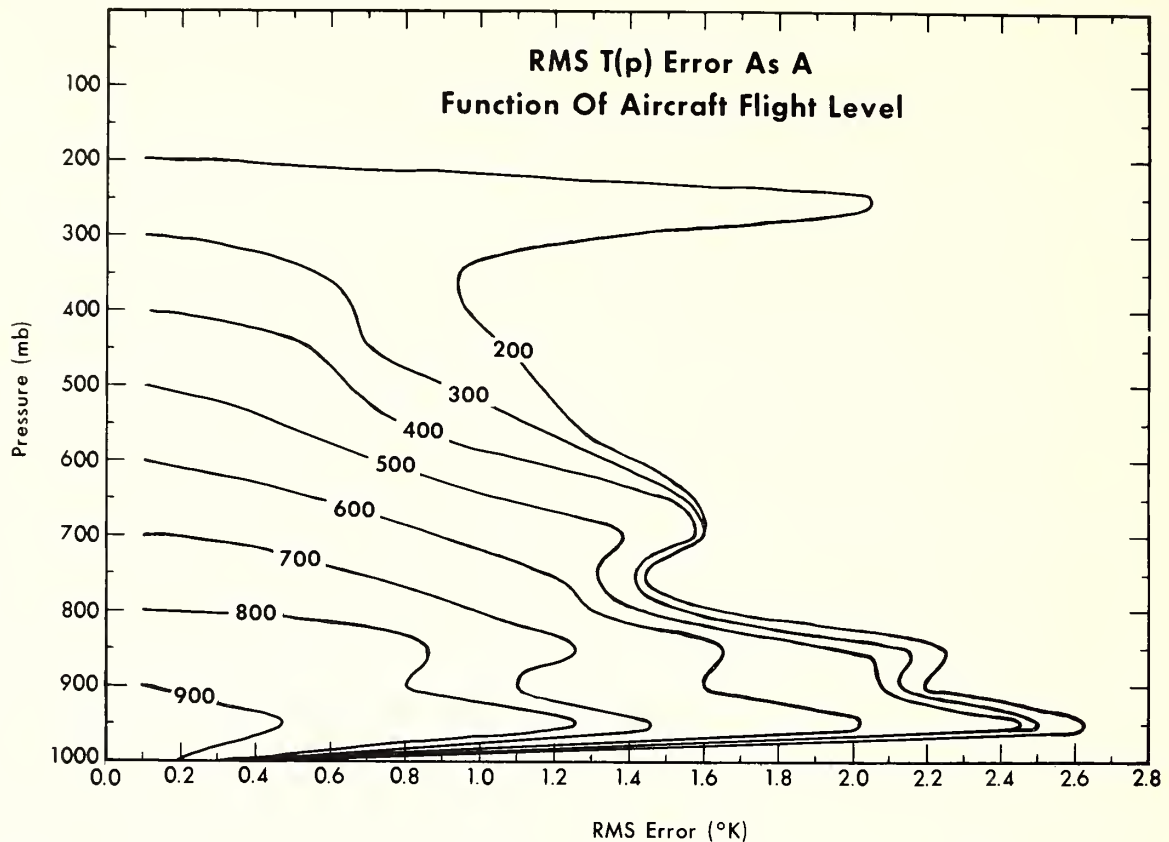


Figure 2.--Standard error of estimate of radiance derived temperature profiles as a function of aircraft flight level

vertical temperature profiles for the dependent sample as a function of the aircraft flight level. As expected, the standard error of estimate for the temperature of a particular pressure level beneath the aircraft decreases with decreasing aircraft altitude (increasing pressure-altitude), especially for the pressure levels near the aircraft pressure-altitude. The standard errors of estimate are largest in the lower troposphere (800-950 mb) where surface inversions occur, and above 300 mb where the tropopause usually exists. The temperature errors are a minimum at the aircraft flight level because the measurement at this level is direct, and are also minimal at the earth's surface because the window channel provides a nearly unique observation of the surface temperature.

B. Total Precipitable Water

To estimate the total precipitable water vapor, U_o , from the 19- μ m water vapor channel radiance, I , the standard iterative equation

$$U_o^{j+1} = U_o^j + \left[\frac{U_o^j - U_o^{j-1}}{\hat{I}^j - \hat{I}^{j-1}} \right] (I - \hat{I}^j) \quad (7)$$

is used. In (7) \hat{I} denotes a calculated radiance and the superscript denotes the iterative step. The precipitable water vapor profile required to

calculate the radiance at each iterative step is given by

$$U(p) = U_0 \left(\frac{p}{p_0} \right)^{\lambda+1} \quad (8)$$

where λ is used at its climatological value of 3.0 (Smith 1966).

C. Clear Column Radiance

When clouds exist, the radiance propagating from the clear air columns must be specified from the measured radiance distribution before soundings down to the earth's surface can be calculated. From an aircraft, one may measure many spatially independent radiances over a short distance along the flight track. Consequently, the variation of the observed radiance over this short distance will be due mainly to variations in the cloudiness within the instrument field of view rather than to variations in atmospheric temperature. If the cloud height is constant over the distance traversed, so that the radiance variations are due to variations in cloud amount, the spatial variation of the radiance in any spectral channel will be linear with respect to the variation of the radiance in any other simultaneously observed spectral channel. This linear function can be used to specify the clear column radiances from the observed cloud contaminated radiance distribution (Smith 1968, Luebke 1971).

To show this, consider the following equation governing the measured radiance $I(v)$ when a cloud fills the fraction N of the instrument's field of view:

$$I(v) = NI_{cd}(v) + (1-N)I_c(v) \quad (9)$$

Here, $I_{cd}(v)$ is the total radiance propagating from all of the cloudy columns of air and $I_c(v)$ is the radiance arising from all of the cloudless columns of air within the instrument field of view. Differentiating (9) with respect to the spatial coordinate, S , assuming $I_{cd}(v)$ and $I_c(v)$ are constant yields

$$\frac{dI(v)}{dS} = \left[I_{cd}(v) - I_c(v) \right] \frac{dN}{dS} \quad (10)$$

Thus it follows that the relation between the radiances observed simultaneously, at two different spectral frequencies, v_i and v_j , is

$$A_1(v_i, v_j) = \frac{I_{cd}(v_i) - I_c(v_i)}{I_{cd}(v_j) - I_c(v_j)} = \frac{dI(v_i)}{dI(v_j)}, \quad (11)$$

where $A_1(v_i, v_j)$ is a constant. Integrating (11) gives

$$I(v_i) = A_0(v_i, v_j) + A_1(v_i, v_j) I(v_j) \quad (12)$$

The coefficients A_0 and A_1 can be determined from a set of simultaneous observations by standard least-squares regression techniques. Then, given clear column radiance for any spectral channel v_j the clear column radiance for any other spectral channel v_i can be predicted from (12).

In practice, the clear column radiance for the window channel is used to predict the clear column radiance for the water vapor and CO_2 channels (see fig. 3). The clear column radiance for the window channel can be obtained from statistical histogram analyses of the window radiance observations (Smith, Rao, Koffler and Curtis 1970) if a sufficient number of cloudless fields of view exist. If no completely cloud-free fields of view are available, the clear column radiance can be specified by horizontal interpolation or from an estimate of the surface temperature, i.e., $I_c = B(T_{\text{sfc}}) + \text{small atmospheric correction}$.

Figure 4 shows the mean and the range (maximum and minimum) of radiances observed from about 35,000 feet within 50 n.mi. sections of an Alaska-to-California flight. Each section consists of 100 spatially independent observations. The clear column radiance profile for the window channel (899 cm^{-1}) was obtained by spatial interpolation of the window radiances obtained from cloud-free fields of view because the horizontal variation is small over the sea. The clear column radiances for the water vapor and carbon dioxide absorption channels were then calculated for each leg using the regression procedure outlined above. These clear column radiances were then used to calculate the temperature and water vapor profiles (shown later).

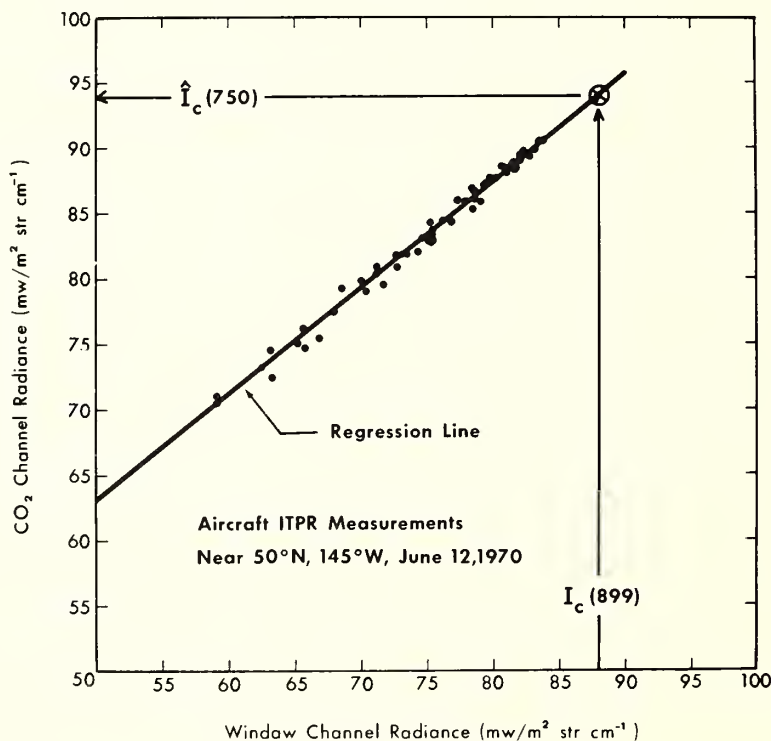


Figure 3.--ITPR measured radiances over a cloudy region. Data for CO_2 channel (750 cm^{-1}) are plotted as a function of data measured in a window channel (899 cm^{-1}).

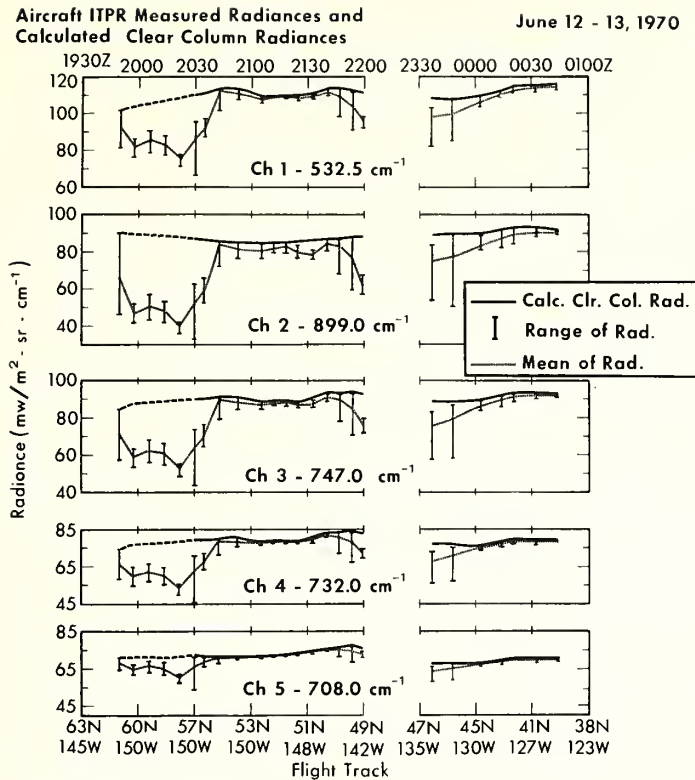


Figure 4.--ITPR measured radiances and calculated clear column radiances from flight over Pacific Ocean, June 12, 1970. The heavy dashed line represents interpolated values between data at first point and at 2030 Z.

D. Cloud Height

Assuming zero cloud reflectivity for the frequency ν_i , it can be shown that

$$I_{cd}(\nu) = \epsilon(\nu) I_{Bcd}(\nu) + [1 - \epsilon(\nu)] I_c(\nu) , \quad (13)$$

where $\epsilon(\nu)$ is the emissivity of the cloud. The "black" cloud radiance is

$$I_{Bcd}(\nu) = B_\nu(p_c) \tau_\nu(p_a, p_c) - \int_{p_a}^{p_c} B_\nu(p) \frac{d\tau_\nu(p_a, p)}{dp} dp , \quad (14)$$

where p_c is the effective cloud pressure. Substituting (13) into (11) gives

$$\frac{dI(\nu_i)}{dI(\nu_j)} = \frac{\epsilon(\nu_i)}{\epsilon(\nu_j)} \left[\frac{I_{Bcd}(\nu_i) - I_c(\nu_i)}{I_{Bcd}(\nu_j) - I_c(\nu_j)} \right] \quad (15)$$

If we choose two frequencies which have approximately the same cloud emissivity (e.g., channels in the wing of the $15\text{-}\mu\text{m}$ CO_2 band) then it follows that

$$\hat{A}_1(v_i, v_j, p_c) = \frac{\hat{I}_{Bcd}(v_i, p_c) - \hat{I}_c(v_i)}{\hat{I}_{Bcd}(v_j, p_c) - \hat{I}_c(v_j)} \quad (16)$$

Given the temperature profile, as calculated from the clear column radiances, \hat{I}_{Bcd} and \hat{I}_c can be calculated using (14) as a function of cloud pressure.

Hence, using (16), the radiance slope $\hat{A}_1(p_c)$ can be calculated as a function of cloud pressure. Then the actual cloud pressure can be specified from the observed slope $A_1(v_i, v_j)$ using the iterative solution

$$p_c^{j+1} = p_c^j + \left[\frac{p_c^j - p_c^{j-1}}{\hat{A}_1(p_c^j) - \hat{A}_1(p_c^{j-1})} \right] \left[A_1(v_i, v_j) - \hat{A}_1(p_c^j) \right], \quad (17)$$

which converges for $A_1(v_i, v_j) \neq 0$. Also, the pressure of a cloud within the field of view of a single observation, within the sample used to determine the clear column radiances, can be specified by letting

$$A_1(v_i, v_j) = \frac{I(v_i) - I_c(v_i)}{I(v_j) - I_c(v_j)} \quad (18)$$

E. Effective Cloud Amount

The effective amount of cloud, N^* (equal to $N \in (v)$), within the instrument field of view can then be specified from one of the two channels used to calculate the cloud pressure using the equation

$$N^* = N \in (v) = \frac{I(v) - I_c(v)}{I_{Bcd}(v) - I_c(v)}, \quad (19)$$

where $I(v)$ is either the mean of a sample of observations or an individual observation, depending upon which was used to specify p_c and consequently $I_{Bcd}(v)$.

4. RESULTS

Figure 5 shows a cross-section of atmospheric temperature obtained while flying at 33,000 feet over a Pacific cold front. The temperature profiles were obtained from the clear column radiances shown in figure 4, using the statistical regression solution presented earlier. The isolines represent departures from the level-mean-values. As shown, the variation of temperature across the front could be diagnosed in this case because there were sufficient breaks in the cloudiness associated with the front.

Figure 6 compares the 1000- to 500-mb and the 500- to 250-mb thickness values obtained from the infrared derived temperature profiles with thickness values derived from simultaneous microwave measurements (NEMS) by Rosenkranz et al. (1971) and observed by the Weather Ship "4YP" (Papa) radiosonde. As

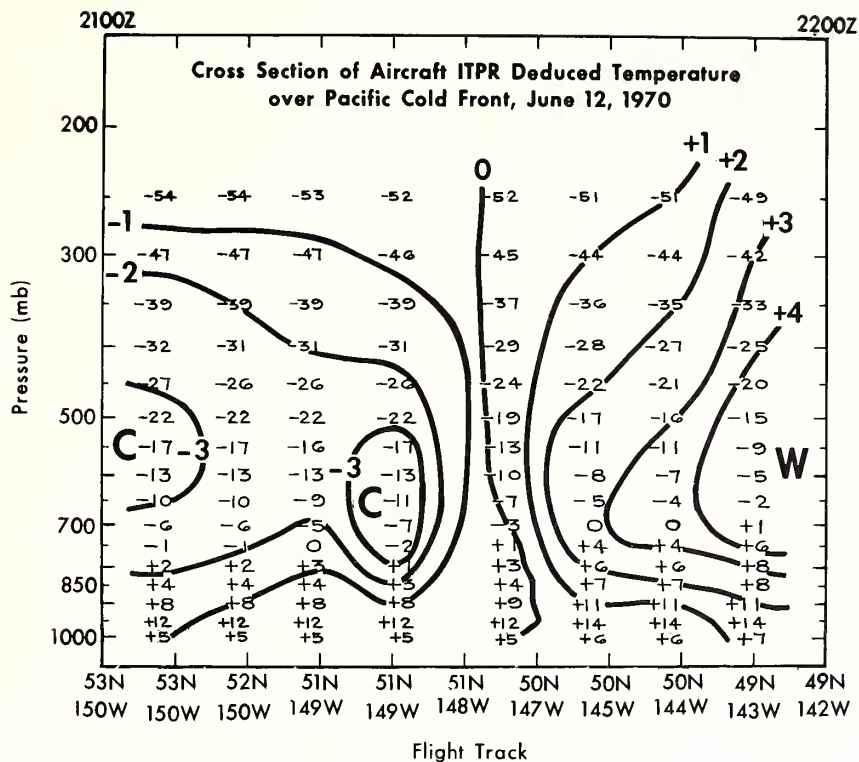


Figure 5.--Cross section of ITPR deduced temperature profiles over Pacific cold front. Isolines show the departure from the level-mean-values.

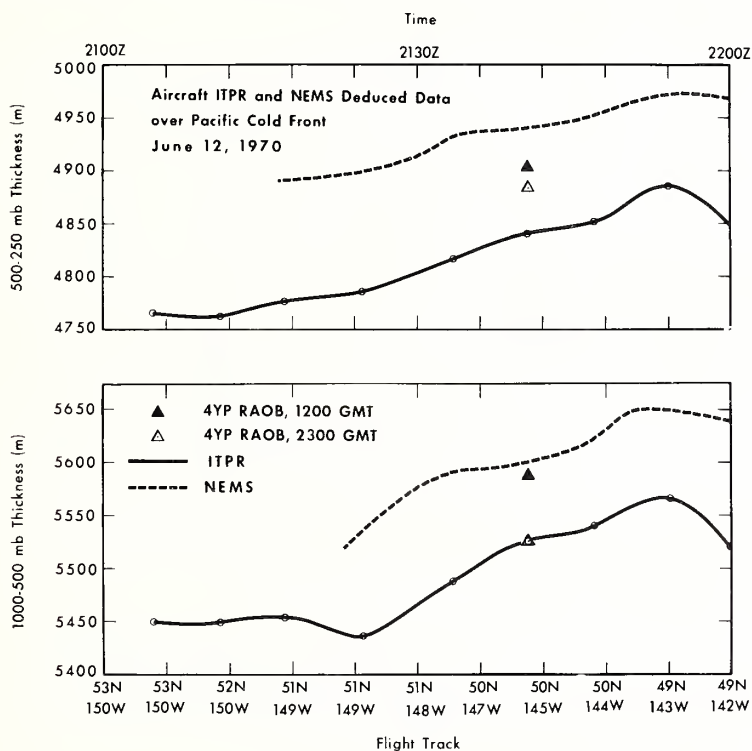


Figure 6.--Thickness values (1000- to 500-mb and 500-mb), derived from infrared measurements, microwave measurements, and 4YP radiosonde data.

shown, there is relatively good agreement between the infrared and the microwave data, although both display some minor discrepancies with the conventional radiosonde data at the location of the weather ship.

Figure 7 compares the total precipitable water vapor derived from the infrared water vapor channel radiance data with that obtained from microwave and radiosonde data. Here we see large discrepancies between the total precipitable water vapor estimates. The systematic discrepancies between the two estimates are clearly related to the temperature discrepancies shown in figure 6. These result because an over estimate (or an under estimate) of temperature requires an over estimate (or under estimate) of water vapor to satisfy a given water vapor channel radiance measurement. The differences in the relative variations through the frontal zone probably are due to the fact that the infrared estimate is only for the clear air column while the microwave estimate includes the water vapor contained within the clouds. This is verified by the two "Papa" raob values, one of which was observed in cloudless air while the other was observed during an ascent through the frontal clouds. The inability of an infrared sensor to sound through clouds is a severe limitation in the sensing of total precipitable water.

Figure 8 shows cloud heights and amounts estimated using two CO_2 channels (as outlined above) and those determined directly from window radiance measurements (i.e., the pressure at which the air temperature was equal to the window channel brightness temperature), and the comparison of both with visual observations. The comparison of the two estimates shows that the window temperature deduced heights are consistently lower, and exhibit a large degree

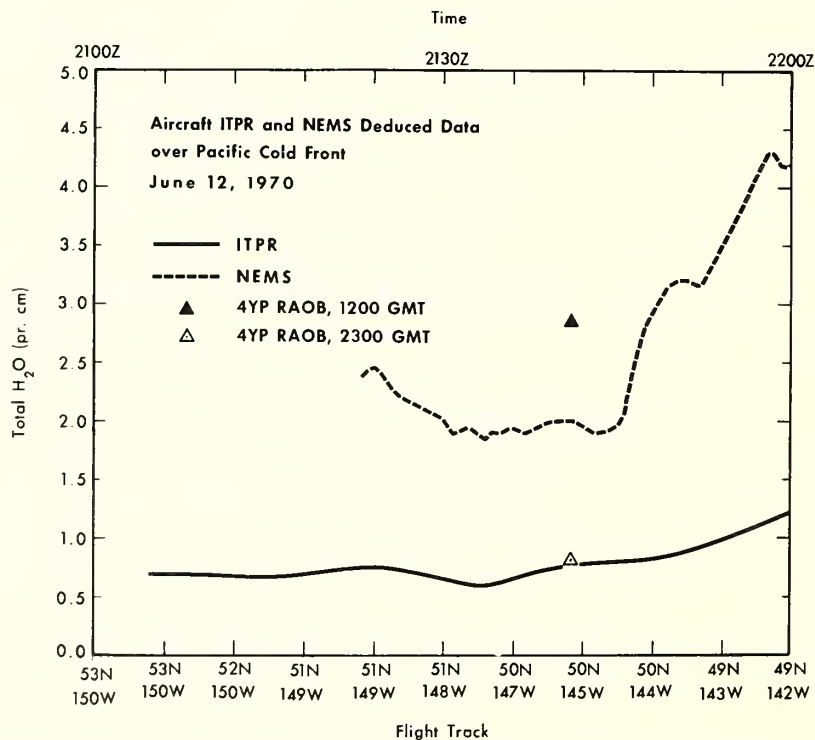


Figure 7.--Total precipitable water vapor derived from infrared, microwave, and 4YP radiosonde data.

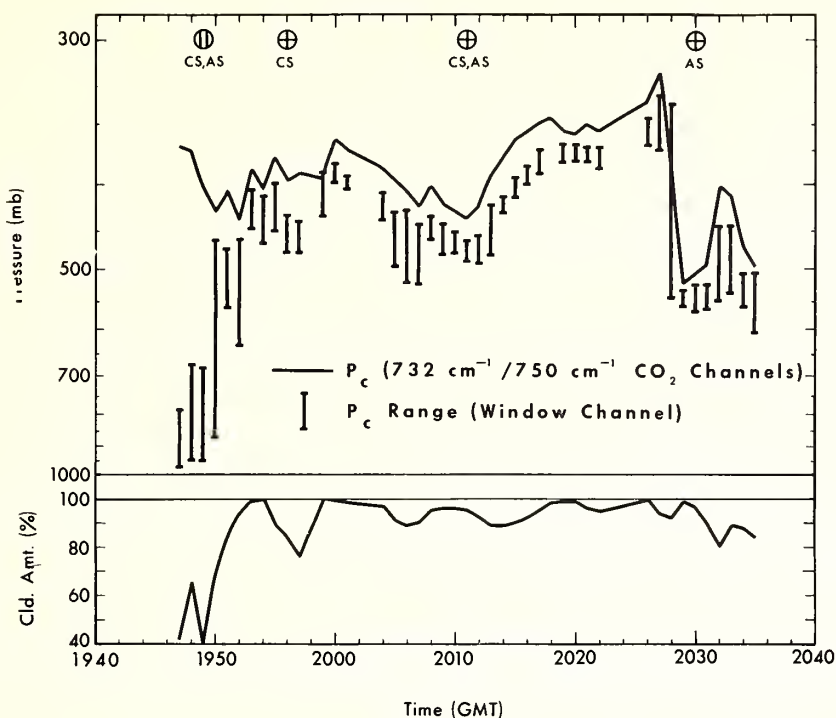


Figure 8.--Estimated cloud top pressure determined from ITPR measured radiances using 732 cm^{-1} and 750 cm^{-1} CO_2 channel observations (solid curve), "window" channel radiance (solid bar) and visual observations (symbols). Shown below is the estimated cloud amount derived from radiances measured in the 732 cm^{-1} and 750 cm^{-1} channels.

of variability even in totally overcast situations. This variability apparently is due to variations in the opacity of the cloud. The measurements in the CO_2 band, on the other hand, provide qualitatively good estimates of the cloud heights, in comparison with corresponding visual observations, even when the field of view is not completely filled with cloud. This is demonstrated by the estimates obtained near the beginning of this flight track. In thick overcast regions, the CO_2 channel estimates display agreement with the maximum heights obtained from window radiances.

5. CONCLUSION

This study shows that multi-spectral infrared radiometers aboard aircraft can be a very effective meteorological observing tool. We propose that this observing capability be used to augment conventional observations for future sub-synoptic scale meteorological research programs, such as the forthcoming GARP Atlantic Tropical Experiment.

ACKNOWLEDGEMENTS

We are grateful for the assistance of L. Mannello, P. Pellegrino, and R. Ryan in the reduction and analysis of the data.

REFERENCES

- Fleming, H. E., and Smith, W. L., "Inversion Techniques for Remote Sensing of Atmospheric Temperature Profiles," presented at the Proceedings of the Fifth Symposium on Temperature, Its Measurement and Control in Science and Industry, Washington, D.C., June 21-24, 1971, to be published 1972.
- Luebbe, R. C., NOAA/National Environmental Satellite Service, 1971, (unpublished notes).
- Rosenkranz, P. W., Staelin, D. H., Barath, F. T., Blinn III, J. C. and Johnson, E. J., "Indirect Sensing of Atmospheric Temperature and Water Vapor Using Microwaves," Proceedings of the Seventh International Symposium on Remote Sensing of Environment, U. of Mich., Vol. III, 1971, pp. 1739-1748.
- Smith, W. L., "Note on the Relationship Between Total Precipitable Water and Surface Dew Point," Journal of Applied Meteorology, Vol. 5, No. 5, Oct. 1966, pp. 726-727.
- Smith, W. L., "An Improved Method for Calculating Tropospheric Temperature and Moisture from Satellite Radiometer Measurements," Monthly Weather Review, Vol. 96, No. 6, June 1968, pp. 387-396.
- Smith, W. L., Rao, P. K., Koffler, R., and Curtis, W. R., "The Determination of Sea-Surface Temperature From Satellite High Resolution Infrared Window Radiation Measurement," Monthly Weather Review, Vol. 98, No. 8, Aug. 1970, pp. 604-611.
- Smith, W. L., Hilleary, D. T., Baldwin, E. C., Jacob, W. R., Jacobowitz, H., Nelson, G., Soules, S. D., and Wark, D. Q., "The Airborne ITPR Brass-board Experiment," NOAA Technical Report NESS 58, Mar. 1972, 74 pp. (Available from the National Technical Information Service.)
- Wark, D. Q., Yamamoto, G., and Lienesch, J., "Methods of Estimating Infrared Flux and Surface Temperature from Meteorological Satellites," Journal of the Atmospheric Sciences, Vol. 19, No. 5, Sept. 1962, pp. 369-384.

(Continued from inside front cover)

- NESC 51 Application of Meteorological Satellite Data in Analysis and Forecasting. Ralph K. Anderson, Jerome P. Ashman, Fred Bittner, Golden R. Farr, Edward W. Ferguson, Vincent J. Oliver, and Arthur H. Smith, September 1969. Price \$1.75 (AD-697-033) Supplement price \$0.65 (AD-740-017)
- NESC 52 Data Reduction Processes for Spinning Flat-Plate Satellite-Borne Radiometers. Torrence H. MacDonald, July 1970. Price \$0.50 (COM-71-00132)
- NESC 53 Archiving and Climatological Applications of Meteorological Satellite Data. John A. Leese, Arthur L. Booth, and Frederick A. Godshall, July 1970. Price \$1.25 (COM-71-00076)
- NESC 54 Estimating Cloud Amount and Height From Satellite Infrared Radiation Data. P. Krishna Rao, July 1970. Price \$0.25 (PB-194-685)
- NESC 56 Time-Longitude Sections of Tropical Cloudiness (December 1966-November 1967). J. M. Wallace, July 1970. Price \$0.50 (COM-71-00131)

NOAA Technical Reports

- NESS 55 The Use of Satellite-Observed Cloud Patterns in Northern Hemisphere 500-mb Numerical Analysis. Roland E. Nagle and Christopher M. Hayden, April 1971. Price \$0.55
- NESS 57 Table of Scattering Function of Infrared Radiation for Water Clouds. Giichi Yamamoto, Masayuki Tanaka, and Shoji Asano, April 1971. Price \$1.00 (COM-71-50312)
- NESS 58 The Airborne ITPR Brassboard Experiment. W. L. Smith, D. T. Hilleary, E. C. Baldwin, W. Jacob, H. Jacobowitz, G. Nelson, S. Soules, and D. Q. Wark, March 1972. Price \$1.25 (COM-72-10557)
- NESS 59 Temperature Sounding From Satellites. S. Fritz, D. Q. Wark, H. E. Fleming, W. L. Smith, H. Jacobowitz, D. T. Hilleary, and J. C. Alishouse, July 1972. Price \$0.55 (COM-72-50963)
- NESS 60 Satellite Measurements of Aerosol Backscattered Radiation From the Nimbus F Earth Radiation Experiment. H. Jacobowitz, W. L. Smith, and A. J. Drummond, August 1972. Price \$0.25 (COM-72-51031)
- NESS 61 The Measurement of Atmospheric Transmittance From Sun and Sky With an Infrared Vertical Sounder. W. L. Smith and H. B. Howell, September 1972. Price \$0.30. (COM-73-50020)
- NESS 62 Proposed Calibration Target for the Visible Channel of a Satellite Radiometer. K. L. Coulson and H. Jacobowitz, October 1972. Price \$0.35
- NESS 63 Verification of Operational SIRS B Temperature Retrievals. Harold Brodrick. January 1973.

PENN STATE UNIVERSITY LIBRARIES



A000072018347